Supplemental Material for "Selective probing of hidden spin-polarized states in inversion-symmetric bulk MoS_2"

E. Razzoli, T. Jaouen, M-L. Mottas, B. Hildebrand, G. Monney, A. Pisoni, S. Muff, M. Fanciulli, N. C. Plumb, V. A. Rogalev, V. N. Strocov, J. Mesot, M. Shi, J. H. Dil, H. Beck, and P. Aebi

January 24, 2017

1 Experimental details

1.1 Photoemission experimental details

The ARPES experiments were performed at the Advanced Resonant Spectroscopies (ADRESS) beamline at the Swiss Light Source (SLS). Data were collected using circularly-polarized light with an overall energy resolution of 50-80 meV. The samples were cleaved in situ at about 25 K and measured in a vacuum always better than 5×10^{-11} mbar. The experimental geometry is described in Ref. [1]. Figure 1 (a)-(f) shows the ARPES intensity maps at various binding energies obtained from our high-quality MoS_2 single crystals. The ARPES intensity maps as a function of energy and $\boldsymbol{k}$ along high symmetry lines are shown in panels (g),(h). The top of the valence band at $\overline{M}$ and $\overline{K}$ is about 1.35, and 0.7 eV below the value at $\overline{\Gamma}$, respectively, in good agreement with the values obtained in our LDA calculations (see Fig. 1 (b) bottom panel in the main text and [2]).

The spin resolved ARPES measurements were performed at the COPHEE end station of SIS beamline [3]. The three-dimensional spin information is obtained by means of two orthogonally oriented classical Mott detectors, each of which measures two spatial components of the photoelectron spin expectation value. All measurements were performed at a base pressure better than 4×10^{-10} mbar, both at 25 K. Incoming light comes at 45°, the sample is tilted 23° degree perpendicularly to the mirror-plane resulting in the angles $\theta_{ph} = 48.3°$ and $\phi_{ph} = 71°$ with respect to the sample surface ($\phi_{ph} = 0°$ for light coming in the plane defined by surface normal and the direction of the outgoing electrons).

2 Theoretical details

2.1 Band structure calculation details

Density functional theory calculations were performed using the linearly augmented plane waves (LAPW) method implemented in the WIEN2K package [4]. Lattice parameters used in the calculation are $a = 3.15$ Å, $c = 12.3$ Å. Spin-orbit interaction is included via a second variational step using the scalar-relativistic eigenfunctions as basis.

2.2 Three step model of Spin-resolved ARPES

The interaction Hamiltonian in presence of radiation is given by:

$$H_{int} = -\frac{e}{cm_e}\mathbf{A}(\mathbf{q}) \cdot \mathbf{p}. \tag{1}$$

The vector potential is $\mathbf{A}(\mathbf{q}) = A\boldsymbol{\epsilon}e^{i\mathbf{q}\cdot\mathbf{r}}$ and in p, s, C_L and C_R polarization $\boldsymbol{\epsilon}$ is given by:

$$\boldsymbol{\epsilon}_p = \begin{pmatrix} -\cos\theta_{ph}\cos\phi_{ph} \\ -\cos\theta_{ph}\sin\phi_{ph} \\ \sin\theta_{ph} \end{pmatrix} \qquad \boldsymbol{\epsilon}_s = \begin{pmatrix} +\sin\phi_{ph} \\ -\cos\phi_{ph} \\ 0 \end{pmatrix} \qquad \boldsymbol{\epsilon}_{C_{R/L}} = \boldsymbol{\epsilon}_p \pm i\boldsymbol{\epsilon}_s \tag{2}$$

For the final state we use the free-electron approximation $\langle\mathbf{r}|\Psi_f\rangle = e^{i\mathbf{p}\cdot\mathbf{r}}|\chi^{\sigma'}_{\mathbf{u}'}\rangle$, while for the initial state we use a tight binding (TB) expansion:

$$\langle\mathbf{r}|\Psi_i\rangle = \frac{1}{\sqrt{N}}\sum_{\gamma,\sigma,\mu,\ell} b^{\sigma}_{i,\mu,\gamma}e^{i\mathbf{k}\cdot\mathbf{R}_\ell}\phi_{\mu,\gamma,\ell}(\mathbf{r})\,|\chi^{\sigma}_{\mathbf{u}}\rangle = \frac{1}{\sqrt{N}}\sum_{\gamma,\sigma,\mu,\ell} b^{\sigma}_{i,\mu,\gamma}e^{i\mathbf{k}\cdot\mathbf{R}_\ell}\phi_{\gamma}\big(\boldsymbol{\mathcal{R}}_\mu(\mathbf{r}-\mathbf{R}_\ell-\mathbf{d}_\mu)\big)\,|\chi^{\sigma}_{\mathbf{u}}\rangle \tag{3}$$

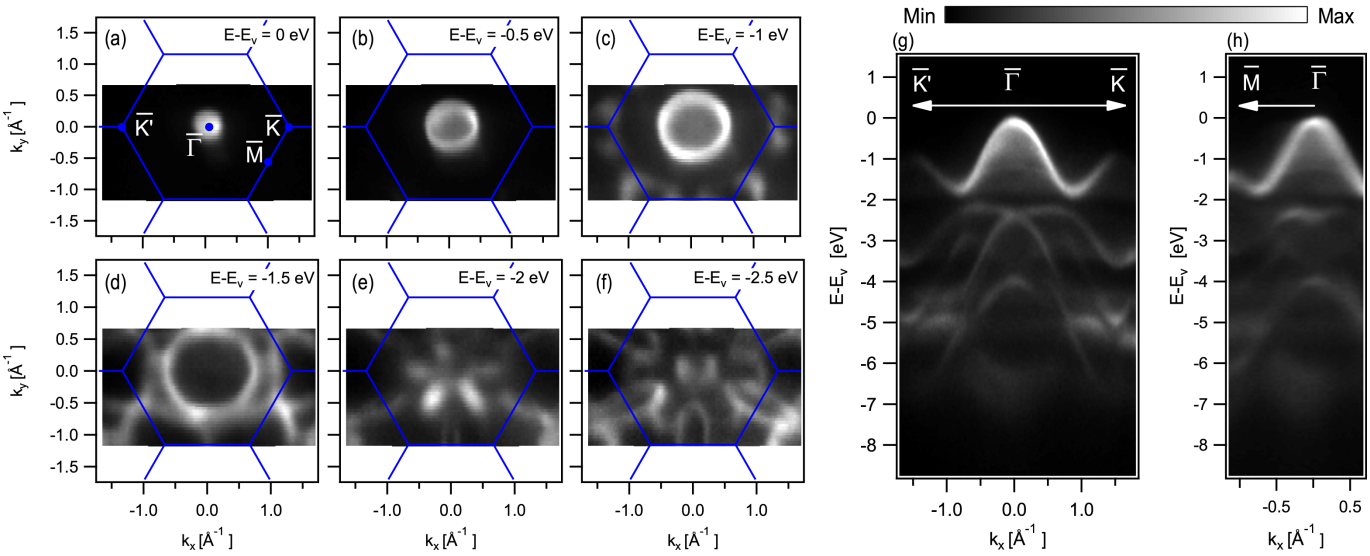

Figure 1: Experimental ARPES intensity maps of MoS_2 acquired at $h\nu = 431$ eV. (a)-(f) Constant binding energy maps map at $E - E_V = 0, -0.5, -1, -1.5, -2, 2.5$ eV, respectively. (g),(h) ARPES spectra along $\overline{K'} - \overline{\Gamma} - \overline{K}$ and $M - \Gamma$ directions.

where $\gamma = (n, l, m_l)$ labels the spherical harmonics, $\phi_\gamma(\mathbf{r}) = R_{n,l}(r)Y_l^{m_l}(\hat{r})$, $\mathbf{R}_\ell$ are the Bravais lattice vectors, the $\mathbf{d}_\mu$ are the position inside the unit cell and $\boldsymbol{\mathcal{R}}_\mu$ is the rotation of frame for the local atom site. In MoS_2, considering only the states coming from Mo atoms, the μ index indicates the layer number.

In the two equations above $\mathbf{u}, \mathbf{u}'$ are versor indicating the quantization directions of the spin on the initial state and on the detector, respectively. In this case the final state momentum inside the crystal is given by:

$$\mathbf{k} = k^{in} \begin{pmatrix} \sin\theta_{in}\cos\phi_{in} \\ \sin\theta_{in}\sin\phi_{in} \\ \cos\theta_{in} \end{pmatrix} \tag{4}$$

with

$$k^{in} = \sqrt{\frac{2m_e}{\hbar^2}\left(\hbar\omega - \phi_{wf} - E_b + V_0\right)}, \qquad k_\parallel^{in} = k_\parallel^{out}, \qquad \phi_{in} = \phi_{out}, \qquad \theta_{in} = \sin^{-1}\left(k_\parallel^{in}/k^{in}\right).$$

For the case of electron emitted from the valence band of MoS_2 surface at the $\bar{K} = (\frac{4\pi}{3a}, 0, k_z(h\nu))$ we use $k_\parallel = \frac{4\pi}{3a}$, $\phi_{in} = 0°$ [5] , $V_0 = 10$ eV (inner potential of the crystal), $E_b = 1.35$ eV, $\phi_{wf} = 4.5$ eV and $\hbar\omega = 50$ eV.

Without losing generality, we consider the $\mathbf{u}$ to be oriented along z and using the Fermi-golden rule gives $I(E_f) \propto \sum_i e^{-\beta E_i} |\langle \Psi_{fin}|H_{int}|\Psi_i\rangle|^2 \delta(E_f - E_i - h\nu)$, the sum on the degenerate initial states i, we find:

$$I_{\sigma',\mathbf{u}'}(\mathbf{k},\mathbf{p},\mathbf{q},E_f) \propto \sum_i e^{-\beta E_i} \left|M_{i,\mathbf{u}'}^{\sigma'}(\mathbf{k},\mathbf{p},\mathbf{q})\right|^2 \delta(E_f - E_i - h\nu) \tag{5}$$

$$\begin{aligned} M_{i,\mathbf{u}'}^{\sigma'}(\mathbf{k},\mathbf{p},\mathbf{q}) &\propto \frac{1}{N}\sum_{\sigma,\gamma,\mu,\ell} b_{i,\mu,\gamma}^{\sigma} e^{i\mathbf{k}\cdot\mathbf{R}_\ell} \langle e^{i\mathbf{p}\cdot\mathbf{r}}\chi_{\mathbf{u}'}^{\sigma'}|\frac{e}{m_e c}\mathbf{A}\cdot\mathbf{p}|\phi_\gamma\big(\boldsymbol{\mathcal{R}}_\mu(\mathbf{r} - \mathbf{R}_\ell - \mathbf{d}_\mu)\big)\chi_z^\sigma\rangle \\ &= \frac{e\hbar}{m_e c}\delta_{\mathbf{p}-\mathbf{q},\mathbf{k}} A\boldsymbol{\epsilon}\cdot\sum_{\sigma,\mu,\gamma} b_{i,\mu,\gamma}^{\sigma} m_{\mathbf{u}',z}^{\sigma',\sigma}\boldsymbol{\kappa}_{\gamma,\mu}(\mathbf{p}-\mathbf{q}) \end{aligned} \tag{6}$$

where:

$$\begin{aligned} m_{\mathbf{u}',z}^{\sigma',\sigma} &= \langle\chi_{\mathbf{u}'}^{\sigma'}|\chi_z^\sigma\rangle = (\underline{\underline{m}}_{\mathbf{u}',z})_{\sigma',\sigma} \\ \underline{\underline{m}}_{\mathbf{u}',z} &= \begin{pmatrix} \cos(\theta_s/2) & e^{i\phi_s}\sin(\theta_s/2) \\ \sin(\theta_s/2) & -e^{i\phi_s}\cos(\theta_s/2) \end{pmatrix} \\ \boldsymbol{\kappa}_{\gamma,\mu}(\mathbf{k}) &= -i\int_\Omega e^{-i\mathbf{k}\cdot\mathbf{r}}\nabla\phi_\gamma\big(\boldsymbol{\mathcal{R}}_\mu(\mathbf{r} - \mathbf{d}_\mu)\big)\,\mathrm{d}^3 r \end{aligned} \tag{7}$$

where (θ_s, ϕ_s) are the polar and azimuthal angles of the finals state spin. Thanks to the relations (in the approximation $\Omega = \Omega''$):

$$\begin{aligned}\boldsymbol{\kappa}_{\gamma,\mu}(\mathbf{k}) &= -ie^{-i\mathbf{k}\cdot\mathbf{d}_\mu}\int_{\Omega'} e^{-i\mathbf{k}\cdot\mathbf{r}'}\nabla\phi_\gamma(\boldsymbol{\mathcal{R}}_\mu\mathbf{r}')\,\mathrm{d}^3r' \\ &= -ie^{-i\mathbf{k}\cdot\mathbf{d}_\mu}\int_{\Omega''} e^{-i\mathbf{k}\cdot\boldsymbol{\mathcal{R}}_\mu^{-1}\mathbf{r}'}\boldsymbol{\mathcal{R}}_\mu^{-1}\nabla\phi_\gamma(\mathbf{r}'')\,\mathrm{d}^3r'' \\ &= e^{-i\mathbf{k}\cdot\mathbf{d}_\mu}\boldsymbol{\mathcal{R}}_\mu^{-1}\boldsymbol{\kappa}_\gamma(\boldsymbol{\mathcal{R}}_\mu\mathbf{k}) \end{aligned} \tag{8}$$

with $\boldsymbol{\kappa}_\gamma(\mathbf{k})$ calculated for $\mathbf{d} = 0$ and $\boldsymbol{\mathcal{R}}_\mu^{-1} = \mathbf{I}$ the above relations give:

$$M^{\sigma'}_{i,\mathbf{u}'}(\mathbf{k}) = \sum_{\sigma,\mu,\gamma} b^\sigma_{i,\mu,\gamma} e^{-i\mathbf{k}\cdot\mathbf{d}_\mu} m^{\sigma',\sigma}_{\mathbf{u}',z}\boldsymbol{\epsilon}\cdot\boldsymbol{\mathcal{R}}_\mu^{-1}\boldsymbol{\kappa}_\gamma(\boldsymbol{\mathcal{R}}_\mu\mathbf{k})$$

where we dropped the constant factor $\frac{e\hbar}{m_e c}A$.

In case of multi-layer structure the influence of the mean free path λ_e can be included by adding an artificial exponential decay of the TB coefficients:

$$b^\sigma_{i,\mu,\gamma} \to b^\sigma_{i,\mu,\gamma}\delta_\mu \quad \mu = 1, 2, .., n_l; \qquad \delta_\mu = e^{-\frac{D(\mu-1)}{\lambda_e}} = \delta^{\mu-1}$$

In this convention $\mu = 1$ is the top layer, $D = c/2$ is the distance between two adjacent layers and $\delta = e^{-D/\lambda_e}$. Thus, including the effect of the mean free path:

$$\boxed{I_{\sigma',\mathbf{u}'}(\mathbf{k}, E_f, h\nu) \propto \sum_i e^{-\beta E_i}\left|M^{\sigma'}_{i,\mathbf{u}'}(\mathbf{k})\right|^2\delta(E_f - E_i - h\nu)} \tag{9}$$

$$\boxed{M^{\sigma'}_{i,\mathbf{u}'}(\mathbf{k}) = \sum_{\sigma,\mu,\gamma} b^\sigma_{i,\mu,\gamma}\delta_\mu e^{-i\mathbf{k}\cdot\mathbf{d}_\mu} m^{\sigma',\sigma}_{\mathbf{u}',z}\boldsymbol{\epsilon}\cdot\boldsymbol{\mathcal{R}}_\mu^{-1}\boldsymbol{\kappa}_\gamma(\boldsymbol{\mathcal{R}}_\mu\mathbf{k})} \tag{10}$$

We note that in the ideal case of $T = 0$, the sum over the initial states in eq. (9) runs over all the degenerate ground states of the system. Interesting, the choice of the initial states is arbitrary since any independent linear combinations of these states are still eigenvectors of the Hamiltonian with the same eigenvalue. However it is easy to show that the I resulting from the eq. (9) is independent of the choice made for the initial states (see 2.10).

2.3 Initial state of MoS_2

Monolayer

The Hamiltonian for MoS_2 mono-layer around the K point, on the basis $\{|d_{z^2}\rangle, \frac{1}{\sqrt{2}}(|d_{x^2-y^2}\rangle + i\tau\,|d_{xy}\rangle)\}$ or equivalently in terms of spherical harmonics $\{|2,0\rangle, |2,\tau 2\rangle\}$ [7] (the radial part is not explicitly given for the moment):

$$\begin{aligned} H =& \begin{pmatrix} \Delta & at(\tau q_x + iq_y) \\ at(\tau q_x - iq_y) & 0 \end{pmatrix} \\ =& at(\tau q_x\widetilde{\sigma_x} - q_y\widetilde{\sigma_y}) + \frac{\Delta}{2}(\widetilde{\sigma_z} + I) \end{aligned} \tag{11}$$

where $\tau = \pm 1$ is the valley index ($+1$ at K, -1 at K'). For $\boldsymbol{q} = 0$ (at K and K') the H is diagonal in the basis, $|2,0\rangle, |2,\tau 2\rangle$ are the eigenfunctions for conduction and valence band, respectively, and Δ is the band-gap. In absence of SO coupling the valence band is spin degenerate.

Including the SO coupling, in the approximation of spherical symmetric potential:

$$H_{so} = \frac{1}{2m_e^2c^2}(\nabla V \times \mathbf{p})\cdot\mathbf{S} = \frac{\hbar}{4m_e^2c^2}\frac{1}{r}\frac{\partial V}{\partial r}(\mathbf{r}\times\mathbf{p})\cdot\boldsymbol{\sigma} \tag{12}$$

the two states $|2,\tau 2,\uparrow\rangle, |2,\tau 2,\downarrow\rangle$ split. To get the Hamiltonian on the basis $\{|2,0,\uparrow\rangle, |2,\tau 2,\uparrow\rangle, |2,0,\downarrow\rangle, |2,\tau 2,\downarrow\rangle\}$ first one evaluates the matrix elements of the radial part of the initial states:

$$H_{so} = \langle R_{42}|H_{so}|R_{42}\rangle = \lambda_{so}\mathbf{L}\cdot\mathbf{S} = \frac{\lambda_{so}\hbar^2}{2}\frac{\mathbf{L}}{\hbar}\cdot\boldsymbol{\sigma} \tag{13}$$

with

$$\lambda_{SO} = \int_0^\infty \mathrm{d}r r^2 \xi_{so}(r)|R_{42}(r)|^2, \qquad \xi_{so}(r) = \frac{1}{2{m_e}^2c^2}\frac{1}{r}\frac{dV(r)}{dr} \quad . \tag{14}$$

The Hamiltonian which includes the spin-orbit coupling of the valence becomes:

$$H = \begin{pmatrix} \Delta & 0 & 0 & 0 \\ 0 & \Delta & 0 & 0 \\ 0 & 0 & +\lambda_{so}\hbar^2\tau & 0 \\ 0 & 0 & 0 & -\lambda_{so}\hbar^2\tau \end{pmatrix} \tag{15}$$

Given that $\langle 2,\tau 2,\downarrow|H'_{so}|2,2\tau\uparrow\rangle = 0$ (so the $|2,2\tau\rangle|\sigma\rangle$ are the good eigenstates for the degenerate perturbation theory), that $\langle 2,\tau 2|L_i|2,2\tau\rangle = 0$ for $i = x,y$ and $\langle 2,2\tau|L_z|2,\tau 2\rangle = 2\tau\hbar$ (see [5]):

$$\begin{aligned} \langle 2,\tau 2,\sigma|H'_{so}|2,\tau 2,\sigma\rangle &= \frac{\lambda_{so}\hbar^2}{2}(2\tau)(\pm 1) \quad \text{for} \quad \sigma = \uparrow,\downarrow \\ \Delta E_{so} &= 2\lambda_{so}\hbar^2 \end{aligned} \tag{16}$$

The valence states closest to E_F are $|2,2,\uparrow\rangle$ and $|2,-2,\downarrow\rangle$ at the K and K' points, respectively. For the photoemission calculation for the top of the valence band for a monolayer we have for the b^σ_γ:

$$\begin{aligned} b^\sigma_{(4,2,-2)} &= 0 \\ b^\sigma_{(4,2,+2)} &= \delta_{\sigma,\uparrow} \end{aligned} \tag{17}$$

at the K point (at K' $b^\sigma_{4,2,-2} = \delta_{\sigma,\downarrow}$, $b^\sigma_{4,2,2} = 0$). This state is non-degenerate and there is just one initial state state which is fully spin polarized and I is directly given by the squared absolute value of eq. (10).

Bi-layer

A bi-layer of MoS_2 can be formed by adding a monolayer rotated by 180° below the original monolayer. Given the rotation, the basis wave functions at K for the lower layer will be the one of the monolayer at K'. For conduction band inter-layer hopping is forbidden by symmetry of the $|2,0\rangle$ orbitals and we can just consider the inter-layer hopping of valence band bases [8]. Using the notation $|l,m\rangle_\mu$ we get:

$$H = \begin{pmatrix} +\lambda_{so}\hbar^2\tau & t_\perp & 0 & 0 \\ t^*_\perp & -\lambda_{so}\hbar^2\tau & 0 & 0 \\ 0 & 0 & -\lambda_{so}\hbar^2\tau & t_\perp \\ 0 & 0 & t^*_\perp & +\lambda_{so}\hbar^2\tau \end{pmatrix} \tag{18}$$

in the basis $\{|2,\tau 2,\uparrow\rangle_1, |2,-\tau 2,\uparrow\rangle_2, |2,\tau 2,\downarrow\rangle_1, |2,-\tau 2,\downarrow\rangle_2\}$. Note that H is block diagonal, implying that spin along z direction is good quantum number.

The eigenvectors of H can be easily calculated and we get that the top of the valence band is doubly degenerate (spin-degeneracy), at K the two degenerate states [8]:

$$\begin{aligned} |n_l = 2, i = 1\rangle &= \frac{1}{\sqrt{2}}\Big(\cos\alpha\,|2,2\rangle_1 + \sin\alpha\,|2,-2\rangle_2\Big)|\uparrow\rangle \\ |n_l = 2, i = 2\rangle &= \frac{1}{\sqrt{2}}\Big(\sin\alpha\,|2,2\rangle_1 + \cos\alpha\,|2,-2\rangle_2\Big)|\downarrow\rangle \end{aligned} \tag{19}$$

with $\cos 2\alpha = \lambda_{so}/\sqrt{\lambda^2_{so} + t^2_\perp}$ and $\mathbf{d}_u = 0$, $\mathbf{d}_l = (\frac{1}{2}a, \frac{2}{3}a, -\frac{1}{2}c)$ and using $\mu = 1$ ($\mu = 2$) for the upper (lower) layer.

This results, for $|n_l = 2, i = 1\rangle$ and $|n_l = 2, i = 2\rangle$, in the following $b^{\sigma}_{i,\mu,\gamma}$:

$$\begin{array}{ll} b^{\sigma}_{1,1,(4,2,-2)} = 0 & b^{\sigma}_{2,1,(4,2,-2)} = 0 \\ b^{\sigma}_{1,1,(4,2,+2)} = \delta_{\sigma,\uparrow}\cos\alpha & b^{\sigma}_{2,1,(4,2,+2)} = \delta_{\sigma,\downarrow}\sin\alpha \\ b^{\sigma}_{1,2,(4,2,-2)} = \delta_{\sigma,\uparrow}\sin\alpha & b^{\sigma}_{2,2,(4,2,-2)} = \delta_{\sigma,\downarrow}\cos\alpha \\ b^{\sigma}_{1,2,(4,2,+2)} = 0 & b^{\sigma}_{2,2,(4,2,+2)} = 0 \end{array} \tag{20}$$

Now, the initial state is doubly degenerate, and in the photoemission intensity of eq. (9) the sum is over two terms.

n_l-layers

In absence of conduction band hopping for n_l layers we have:

$$H = \begin{pmatrix} H_{\uparrow} & 0 \\ 0 & H_{\downarrow} \end{pmatrix} \tag{21}$$

$$H_{\uparrow} = \begin{pmatrix} +\lambda_{so}\hbar^2\tau & t_{\perp}^{12} & t_{\perp}^{13} & ... & t_{\perp}^{1n} \\ t_{\perp}^{12^*} & -\lambda_{so}\hbar^2\tau & t_{\perp}^{23} & ... & t_{\perp}^{2n} \\ t_{\perp}^{13^*} & t_{\perp}^{23^*} & +\lambda_{so}\hbar^2\tau & ... & t_{\perp}^{3n} \\ ... & ... & ... & ... & ... \\ t_{\perp}^{1n^*} & t_{\perp}^{2n^*} & t_{\perp}^{3n^*} & ... & (-1)^{(n_l+1)}\lambda_{so}\hbar^2\tau \end{pmatrix} \tag{22}$$

$$H_{\downarrow} = \begin{pmatrix} -\lambda_{so}\hbar^2\tau & t_{\perp}^{12} & t_{\perp}^{13} & ... & t_{\perp}^{1n} \\ t_{\perp}^{12^*} & +\lambda_{so}\hbar^2\tau & t_{\perp}^{23} & ... & t_{\perp}^{2n} \\ t_{\perp}^{13^*} & t_{\perp}^{23^*} & -\lambda_{so}\hbar^2\tau & ... & t_{\perp}^{3n} \\ ... & ... & ... & ... & ... \\ t_{\perp}^{1n^*} & t_{\perp}^{2n^*} & t_{\perp}^{3n^*} & ... & (-1)^{n_l}\lambda_{so}\hbar^2\tau \end{pmatrix} \tag{23}$$

The matrices can be easily diagonalized numerically (we use $t_{\perp}^{\mu,\mu'} = \delta_{\mu',\mu\pm1}t_{\perp}$). Given the block diagonal form the eigenstates are either fully spin up or spin down. In case of n_l even each state with spin up has a corresponding state with spin down at the same energy. So the top of the valence band is still doubly degenerate, as it should be in the bulk system. The state at higher energy (E_{max}) is the one with the coefficients of the eigenvector of the same sign (corresponding to $k_z = 0$ point in a tight binding picture). The coefficients are give in terms of the eigenvector components $a^{\uparrow}_{\mu}, a^{\downarrow}_{\mu}$ of $H^{\uparrow}$ and $H^{\downarrow}$ corresponding to the eigenvalue E_{max}:

$$\begin{array}{ll} b^{\sigma}_{1,1,(4,2,-2)} = 0 & b^{\sigma}_{2,1,(4,2,-2)} = 0 \\ b^{\sigma}_{1,1,(4,2,+2)} = \delta_{\sigma,\uparrow}a^{\uparrow}_1 & b^{\sigma}_{2,1,(4,2,+2)} = \delta_{\sigma,\downarrow}a^{\downarrow}_1 \\ b^{\sigma}_{1,2,(4,2,-2)} = \delta_{\sigma,\uparrow}a^{\uparrow}_2 & b^{\sigma}_{2,2,(4,2,-2)} = \delta_{\sigma,\downarrow}a^{\downarrow}_2 \\ b^{\sigma}_{1,2,(4,2,+2)} = 0 & b^{\sigma}_{2,2,(4,2,+2)} = 0 \\ ... & ... \\ ... & ... \\ b^{\sigma}_{1,n_l,(4,2,-2)} = \delta_{\sigma,\uparrow}a^{\uparrow}_{n_l} & b^{\sigma}_{2,n_l,(4,2,-2)} = \delta_{\sigma,\downarrow}a^{\downarrow}_{n_l} \\ b^{\sigma}_{1,n_l,(4,2,+2)} = 0 & b^{\sigma}_{2,n_l,(4,2,+2)} = 0 \end{array} \tag{24}$$

2.4 Evaluation of Matrix element integrals

We are then left with the problem of obtaining $\boldsymbol{\kappa}_{\gamma}(\mathbf{k})$ at $\mathbf{k}$ given by eq. (4). Now by using the relation $\nabla = -\frac{m_e}{\hbar^2}[H, \mathbf{r}]$ and the spherical harmonics expansion of the initial state $\phi_{\gamma}(\mathbf{r})$, of the final state $e^{i\mathbf{k}\cdot\mathbf{r}}$:

$$e^{-i\mathbf{k}\cdot\mathbf{r}} = 4\pi \sum_{l_k, m_k} (-i)^{l_k} j_{l_k}(kr) Y_{l_k}^{m_k *}(\hat{r}) Y_{l_k}^{m_k}(\hat{k}), \tag{25}$$

and of the position operator:

$$\mathbf{r} = \sqrt{\frac{4\pi}{3}} r \begin{pmatrix} \frac{1}{\sqrt{2}}\left[Y_1^{-1}(\hat{r}) - Y_1^{+1}(\hat{r})\right] \\ \frac{i}{\sqrt{2}}\left[Y_1^{-1}(\hat{r}) + Y_1^{+1}(\hat{r})\right] \\ Y_1^0(\hat{r}) \end{pmatrix} \tag{26}$$

we can rewrite the vector $\boldsymbol{\kappa}_{\gamma}(\mathbf{k})$, as function of the parameters $\kappa^{\nu}_{n,l,m}(\mathbf{k})$, ($\nu = -1, 0, 1$):

$$\kappa^{\nu}_{n,l,m}(\mathbf{k}) = 4\pi i \sum_{l_k,m_k} (-i)^{l_k}(-1)^{m_k} Y^{m_k}_{l_k}(\hat{k}) g(l,m,l_k,-m_k,1,\nu)\rho^{l_k}_{n,l}(k) \tag{27}$$

$$\rho^{l_k}_{n,l}(k) = \sqrt{\frac{4\pi}{3}}\frac{m_e\omega}{\hbar}\int r^3 j_{l_k}(kr)R_{n,l}(r)\,\mathrm{d}r \tag{28}$$

$$\boldsymbol{\kappa}_{\gamma}(\mathbf{k}) = \begin{pmatrix} \frac{1}{\sqrt{2}}\left[\kappa^{\nu=-1}_{\gamma}(\mathbf{k}) - \kappa^{\nu=+1}_{\gamma}(\mathbf{k})\right] \\ \frac{i}{\sqrt{2}}\left[\kappa^{\nu=-1}_{\gamma}(\mathbf{k}) + \kappa^{\nu=+1}_{\gamma}(\mathbf{k})\right] \\ \kappa^{\nu=0}_{\gamma}(\mathbf{k}) \end{pmatrix} \tag{29}$$

In this equation $j_{l_k}(kr)$ are the spherical Bessel functions and $g(l,m,l_k,m_k,L,M)$ are the Gaunt coefficients defined according to eq. (46).

2.5 Radial-part parameters

For the initial state of a single layer of MoS_2 $|R_{42}\rangle\,|2,\tau 2\rangle$ we have to fix the radial part to evaluate the radial integrals. To do so we approximate the potential as a Yukawa potential:

$$V(r) = -ZV_0\frac{e^{-\frac{r}{d}}}{r} \tag{30}$$

where $V_0 = \frac{e^2}{4\pi\epsilon_0}$. The advantage of this approximation is that the eigenstates of Yukawa potential can be calculated analytically [9]. The free parameters in V are obtained demanding that the λ_{SO} in eq. (14)-(16) matches the value obtained from first principle calculations. Using $Z = 21$ and $d = 0.65\ a_{bohr}$ we have $\lambda_{so}\hbar^2 = 73$ meV, the same value obtained from LDA calculations [5]. With this values we get $\rho \equiv \dfrac{\rho^3_{4,2}}{\rho^1_{4,2}} = 1.8$.

2.6 Spin flipping transition in the final states

Final states spin flips can be induced by the interacting Hamiltonian $H^{SO}_{int} = -\frac{e\hbar}{m_e c}\mathbf{A}(\mathbf{q})\cdot\frac{1}{4m_e c^2 r}\frac{\partial V}{\partial r}(\boldsymbol{\sigma}\times\mathbf{r})$ obtained by the Peierls substitution in the H_{SO} given in eq. (12). Using the substitution eq. (26), the matrix elements can be evaluated similarly to the ones for $\mathbf{A}\cdot\mathbf{r}$ and the radial part is given by

$$\beta^{l_k}_{n,l}(k) = \sqrt{\frac{4\pi}{3}}\frac{1}{4m_e c^2}\int r^2\frac{\partial V}{\partial r}j_{l_k}(kr)R_{n,l}(r)\,\mathrm{d}r \tag{31}$$

The ratio ρ/β can be estimated by comparing the terms differing in the two expressions, i.e., $r^3\frac{m_e\omega}{\hbar}$ and $r^2\frac{\partial V}{\partial r}\frac{1}{4m_e c^2}$. For the first term, since the cut off of the integral is of the order of a_{Bohr} (given by $R_{4,2}$) r^3 is of the order of a^3_{Bohr} in that interval. For the Yukawa potential in eq. (30) $r^2\frac{\partial V}{\partial r} \approx ZV_0$. Using this two values the ratio ρ/β is of the order of 10^6, suggesting that the contribution of H^{SO}_{int} to the photoemission intensity is negligible. Calculations using the analytic solutions of the Yukawa potential give $\beta^1_{4,2}/\rho^3_{4,2} = 2\times10^{-5}$ and $\beta^3_{4,2}/\rho^3_{4,2} = 8\times10^{-6}$ in good agreement with our estimate.

2.7 MoS_2 bilayer at normal incidence

For MoS_2, given that $\boldsymbol{\mathcal{R}}^{-1}_{\mu}\boldsymbol{\kappa}_{\gamma}(\boldsymbol{\mathcal{R}}_{\mu}\mathbf{k}) = \boldsymbol{\kappa}_{\gamma}(\mathbf{k})$ and excluding spin flip transition in the final state, the photoemision intensity is diagonal in the spin index, and can be written as:

$$I^{\boldsymbol{\epsilon}}_{\sigma',z} \propto \Sigma_i|\Sigma_{\gamma}\eta^{\sigma'}_{i,\gamma}\boldsymbol{\kappa}_{\gamma}\cdot\boldsymbol{\epsilon}|^2$$

with $\eta^{\sigma'}_{i,\gamma} = \Sigma_{\mu}b^{\sigma'}_{i,\mu,\gamma}\delta_{\mu}e^{-i\mathbf{k}\cdot\mathbf{d}_{\mu}}$. For MoS_2 bilayer using eq. (20) we find:

$$I^{\boldsymbol{\epsilon}}_{\uparrow,z} \propto |\cos(\alpha)\boldsymbol{\kappa}_{2,2}\cdot\boldsymbol{\epsilon} + \sin(\alpha)\delta e^{-i\mathbf{k}\cdot\mathbf{d}_l}\boldsymbol{\kappa}_{2,-2}\cdot\boldsymbol{\epsilon}|^2 \tag{32}$$

$$I^{\boldsymbol{\epsilon}}_{\downarrow,z} \propto |\sin(\alpha)\boldsymbol{\kappa}_{2,2}\cdot\boldsymbol{\epsilon} + \cos(\alpha)\delta e^{-i\mathbf{k}\cdot\mathbf{d}_l}\boldsymbol{\kappa}_{2,-2}\cdot\boldsymbol{\epsilon}|^2 \tag{33}$$

Direct calculation of the $\boldsymbol{\kappa}$ from eq. (27)-(29) gives for $l = 2, m = \pm 2$:

$$\boldsymbol{\kappa}_{l,m} = \Sigma_{l',m'} C_{l,l'}^{m,m'} \mathbf{e}_{m,m'}, \qquad \mathbf{e}_{m,m\mp1} = \begin{pmatrix} 1 \\ \pm i \\ 0 \end{pmatrix}, \quad \mathbf{e}_{m,m} = \begin{pmatrix} 0 \\ 0 \\ 1 \end{pmatrix} \tag{34}$$

with $C_{l,l'}^{m,m'} = C_{l,l'}^{-m,-m'}$ and $C_{l,l'}^{m,m'} \neq 0$ only for $l' = l \pm 1, m' = m, m \pm 1$ and $|m'| \leq l'$, in agreement with selection rules for electric dipole transitions. At normal emission $\mathbf{e}_{m,m'} \cdot \boldsymbol{\epsilon}^{\mathbf{n}}_{C_{R/L}} \propto \delta_{m,m\pm1}$ and thus $m' - m = \pm 1$ for C_R and C_L, respectively, as required by the conservation of total angular momentum. In case of light coming at normal incidence we have:

$$\begin{array}{ll}
\boldsymbol{\kappa}_{2,2} \cdot \boldsymbol{\epsilon}^{\mathbf{n}}_{p} = -[C_{2,1}^{2,1} + C_{2,3}^{2,1} + C_{2,3}^{2,3}] & \boldsymbol{\kappa}_{2,-2} \cdot \boldsymbol{\epsilon}^{\mathbf{n}}_{p} = -[C_{2,1}^{-2,-1} + C_{3}^{-2,-1} + C_{2,3}^{-2,-3}] = \boldsymbol{\kappa}_{2,2} \cdot \boldsymbol{\epsilon}^{\mathbf{n}}_{p} \\
\boldsymbol{\kappa}_{2,2} \cdot \boldsymbol{\epsilon}^{\mathbf{n}}_{s} = -i[C_{2,1}^{2,1} + C_{2,3}^{2,1} - C_{2,3}^{2,3}] & \boldsymbol{\kappa}_{2,-2} \cdot \boldsymbol{\epsilon}^{\mathbf{n}}_{s} = -i[C_{2,3}^{-2,-3} - C_{2,1}^{-2,-1} - C_{2,3}^{-2,-1}] \\
\boldsymbol{\kappa}_{2,2} \cdot \boldsymbol{\epsilon}^{\mathbf{n}}_{C_R} = -2[C_{2,3}^{2,3}] & \boldsymbol{\kappa}_{2,-2} \cdot \boldsymbol{\epsilon}^{\mathbf{n}}_{C_R} = -2[C_{2,1}^{-2,-1} + C_{2,3}^{-2,-1}] = \boldsymbol{\kappa}_{2,2} \cdot \boldsymbol{\epsilon}^{\mathbf{n}}_{C_L} \\
\boldsymbol{\kappa}_{2,2} \cdot \boldsymbol{\epsilon}^{\mathbf{n}}_{C_L} = -2[C_{2,1}^{2,1} + C_{2,3}^{2,1}] & \boldsymbol{\kappa}_{2,-2} \cdot \boldsymbol{\epsilon}^{\mathbf{n}}_{C_L} = -2[C_{2,3}^{-2,-3}] = \boldsymbol{\kappa}_{2,2} \cdot \boldsymbol{\epsilon}^{\mathbf{n}}_{C_R}
\end{array} \tag{35}$$

The C coefficients can be written more explicitly as $C_{l,l'}^{m,m'} = c_{l,l'}^{m,m'} Y_{l'}^{m'}(\hat{k})$ and:

$$\begin{aligned}
c_{l,l'}^{m,m\pm1} &= \frac{4\pi i}{\sqrt{2}} (-i)^{l'} (-1)^{m\pm1} \rho_{n,l}^{l'}(\hat{k}) \big[g\big(l, m, l', -(m \pm 1), 1, -1\big) - g\big(l, m, l', -(m \pm 1), 1, 1\big) \big] \\
c_{l,l'}^{m,m} &= 4\pi i (-i)^{l'} (-1)^{m} \rho_{n,l}^{l'}(\hat{k}) g(l, m, l', -m, 1, 0)
\end{aligned} \tag{36}$$

The values of the $c_{2,l'}^{2,m'}$ are given by:

l' \ m'	1	2	3
1	$-\sqrt{\frac{12\pi}{5}}\rho_{4,2}^{1}$	0	0
3	$-\sqrt{\frac{6\pi}{35}}\rho_{4,2}^{3}$	$-\sqrt{\frac{12\pi}{7}}\rho_{4,2}^{3}$	$\sqrt{\frac{18\pi}{7}}\rho_{4,2}^{3}$

For electrons at the K point we obtain $C_{2,1}^{2,1} = 0.33$, $C_{2,3}^{2,1} = 0.51, C_{2,3}^{2,2} = -0.49$ and $C_{2,3}^{2,3} = -0.09$ (in unit of $\rho_{4,2}^{1}$). Noticing that $C_{2,3}^{2,3} \ll (C_{2,1}^{2,1} + C_{2,3}^{2,1})$ we get that $|\boldsymbol{\kappa}_{2,\mp2} \cdot \boldsymbol{\epsilon}^{\mathbf{n}}_{C_{R/L}}| \gg |\boldsymbol{\kappa}_{2,\pm2} \cdot \boldsymbol{\epsilon}^{\mathbf{n}}_{C_{R/L}}|$ and equations (32)-(33) simplifies in:

$$\begin{array}{ll}
I_{\uparrow,z}^{C_R} \approx 4\sin^2(\alpha)\delta^2(C_1^1 + C_3^1)^2 & I_{\downarrow,z}^{C_R} \propto 4\cos^2(\alpha)\delta^2(C_1^1 + C_3^1)^2 \\
I_{\uparrow,z}^{C_L} \approx 4\cos^2(\alpha)(C_1^1 + C_3^1)^2 & I_{\downarrow,z}^{C_L} \propto 4\sin^2(\alpha)(C_1^1 + C_3^1)^2
\end{array}$$

Thus in case of normal incident light we obtain:

$$P_z^{C_{R/L}} \approx \mp\Big(\cos^2(\alpha) - \sin^2(\alpha) \Big) = \mp \cos 2\alpha. \tag{37}$$

The interpretation of this formula is quite simple. Taking for example the case of C_R light, the electron photoemitted must have an initial $m = -2$. Based on eq. (19) most of them (proportionally to $\cos^2\alpha$) have spin down while the rest (proportionally to $\sin^2\alpha$) have spin up.

2.8 Interference effects

The possibility of coherent interference between distinct degenerate initial states is not included in our analysis of the photoemission process. The summation in eq. (9) over degenerate initial state is indeed carried out in incoherent way, and only interference within the same state, such as interference between different layers, is included. On the one hand, given that the initial states of n_l-layers are purely spin up and down along z, and that H_{int} conserves the spin, taking the coherent sum, i.e. summing the initial states before performing the modulus square, doesn't affect the calculation of P_z. In fact, for even number of layers:

$$I_{\uparrow(\downarrow),z} \propto \Big| \langle e^{i\mathbf{k}\cdot\mathbf{r}}, \uparrow(\downarrow) | H_{int} | 1 \rangle + \langle e^{i\mathbf{k}\cdot\mathbf{r}}, \uparrow(\downarrow) | H_{int} | 2 \rangle \Big|^2 = \Big| \langle e^{i\mathbf{k}\cdot\mathbf{r}} | H_{int} | u(v) \rangle \Big|^2 \tag{38}$$

where we used the notation $|1\rangle = |u\rangle|\uparrow\rangle$ and $|2\rangle = |v\rangle|\downarrow\rangle$. For the bilayer, the above result is equivalent to eq. (32), (33) and results in $P_z^{C_{R/L}} \approx \mp\cos 2\alpha$, once the $|u\rangle$ and $|u\rangle$ from equation (19) are used. On the other hand, the coherent summation results in a non vanishing $P_\parallel$. In particular, we still have $I_{\uparrow,y} = I_{\downarrow,y}$ but now:

$$\begin{aligned} I_{\uparrow(\downarrow),x} &\propto \left| \langle e^{i\mathbf{k}\cdot\mathbf{r}}|H_{int}|u\rangle \langle\uparrow_x (\downarrow_x)| \uparrow\rangle + \langle e^{i\mathbf{k}\cdot\mathbf{r}}|H_{int}|v\rangle \langle\uparrow_x (\downarrow_x)| \downarrow\rangle \right|^2 \\ &= \frac{1}{2}\left| \langle e^{i\mathbf{k}\cdot\mathbf{r}}|H_{int}|u\rangle \pm \langle e^{i\mathbf{k}\cdot\mathbf{r}}|H_{int}|v\rangle \right|^2. \end{aligned} \tag{39}$$

Using these results for calculating P_x with circular light at normal incidence with $|\boldsymbol{\kappa}_{2,\mp 2}\cdot\boldsymbol{\epsilon}^{\mathbf{n}}_{C_{R/L}}| \gg |\boldsymbol{\kappa}_{2,\pm 2}\cdot\boldsymbol{\epsilon}^{\mathbf{n}}_{C_{R/L}}|$ we obtain:

$$P_x^{C_{R/L}} \approx \sin 2\alpha. \tag{40}$$

For the bilayer calculations shows that $\cos 2\alpha = 0.863$ [8], and thus our simple calculation at normal emission would predict $P_z = 0.86$ and $P_x = 0.26$, not far from the our experimental observation (see Fig. 2).

Another possible source of interference could be related to modification of eigenstates of the monolayer. In an unperturbed MoS_2 monolayer the VB1 eigenstates at K and K' are $|2, 2, \uparrow\rangle$ and $|2, -2, \downarrow\rangle$, respectively. However perturbation like mirror symmetry breaking induced by a substrate or VB1-VB2 interband impurity scattering can modify the eigenstate resulting in a phenomenological eigenstate:

$$|n_l = 1, K\rangle = A\Big(|2, 2\rangle \left(|\uparrow\rangle + a\,|\downarrow\rangle \right) + b\,|2, -2\rangle \left(|\downarrow\rangle + c\,|\uparrow\rangle \right) \Big) \tag{41}$$

where $b = 0$ with preserved mirror symmetry (σ_h) and $a = c = 0$ in absence of interlayer mixing due to scattering. Note that spin along z on a given layer is opposite for VB1 and VB2 as given by the SO interaction. These terms can give rise to interference of spin states and can thus be a source of rotation of the spin polarization vector measured by spin resolved ARPES [6]. In the simple case of bilayer, focusing on the interband mixing only we get:

$$\begin{aligned} |n_l = 2, i = 1, a\rangle &= A\Big(\cos\alpha\,|2, 2\rangle_1 \left(|\uparrow\rangle + a_{1,1}\,|\downarrow\rangle \right) + \sin\alpha\,|2, -2\rangle_2 \left(|\uparrow\rangle + a_{1,2}\,|\downarrow\rangle \right) \Big) \\ |n_l = 2, i = 2, a\rangle &= A\Big(\sin\alpha\,|2, 2\rangle_1 \left(|\downarrow\rangle + a_{2,1}\,|\uparrow\rangle \right) + \cos\alpha\,|2, -2\rangle_2 \left(|\downarrow\rangle + a_{2,2}\,|\uparrow\rangle \right) \Big) \end{aligned} \tag{42}$$

where $a_{i,\mu}$ is proportional to the mixing of VB1 state i with states from VB2 on the layer μ. In this case equations (32) and (33) are modified since the I is not any more diagonal in the spin index and we obtain:

$$\begin{aligned} I^{\boldsymbol{\epsilon}}_{\uparrow,z} &= I^{1,\boldsymbol{\epsilon}}_{\uparrow,z} + I^{2,\boldsymbol{\epsilon}}_{\uparrow,z} \propto |\cos(\alpha)\boldsymbol{\kappa}_{2,2}\cdot\boldsymbol{\epsilon} + \sin(\alpha)\delta e^{-i\mathbf{k}\cdot\mathbf{d}_l}\boldsymbol{\kappa}_{2,-2}\cdot\boldsymbol{\epsilon}|^2 + |a_{2,1}\sin(\alpha)\boldsymbol{\kappa}_{2,2}\cdot\boldsymbol{\epsilon} + a_{2,2}\cos\alpha\delta e^{-i\mathbf{k}\cdot\mathbf{d}_l}\boldsymbol{\kappa}_{2,-2}\cdot\boldsymbol{\epsilon}|^2 \\ I^{\boldsymbol{\epsilon}}_{\downarrow,z} &= I^{1,\boldsymbol{\epsilon}}_{\downarrow,z} + I^{2,\boldsymbol{\epsilon}}_{\downarrow,z} \propto |a_{1,1}\cos(\alpha)\boldsymbol{\kappa}_{2,2}\cdot\boldsymbol{\epsilon} + a_{1,2}\sin(\alpha)\delta e^{-i\mathbf{k}\cdot\mathbf{d}_l}\boldsymbol{\kappa}_{2,-2}\cdot\boldsymbol{\epsilon}|^2 + |\sin(\alpha)\boldsymbol{\kappa}_{2,2}\cdot\boldsymbol{\epsilon} + \cos(\alpha)\delta e^{-i\mathbf{k}\cdot\mathbf{d}_l}\boldsymbol{\kappa}_{2,-2}\cdot\boldsymbol{\epsilon}|^2 \end{aligned} \tag{43}$$

In the approximation $a_{i,\mu} \approx a$ the P_z for circular light at normal emission is:

$$P_z^{C_{R/L}} \approx \mp\frac{1-|a|^2}{1+|a|^2}\cos 2\alpha. \tag{44}$$

Thus, since $(1-|a|^2)/(1+|a|^2) \approx 1-|a|^2$ for $|a| \ll 1$, interference correction to the P_z are of order of $|a|^2$ and can be neglected. With the assumption of a real a, i.e. of an in-phase coherent mixing of the state in VB1 and VB2 we get $P_y^{C_{R/L}} = 0$ and:

$$P_x^{C_{R/L}} \approx \frac{2a}{1+2a^2} \tag{45}$$

where we used the relations $|\uparrow\rangle + a\,|\downarrow\rangle = \frac{1+a}{\sqrt{2}}|\uparrow_x\rangle + \frac{1-a}{\sqrt{2}}|\downarrow_x\rangle$ and $|\downarrow\rangle + a\,|\uparrow\rangle = \frac{1+a}{\sqrt{2}}|\uparrow_x\rangle - \frac{1-a}{\sqrt{2}}|\downarrow_x\rangle$. The induced P_x is of order of a and thus is not negligible. For $a \approx 0.1$ correction to P_z are about 1% while P_x in increased from 0 to 0.2, in qualitative agreement with our experimental observation (see Fig. 2).

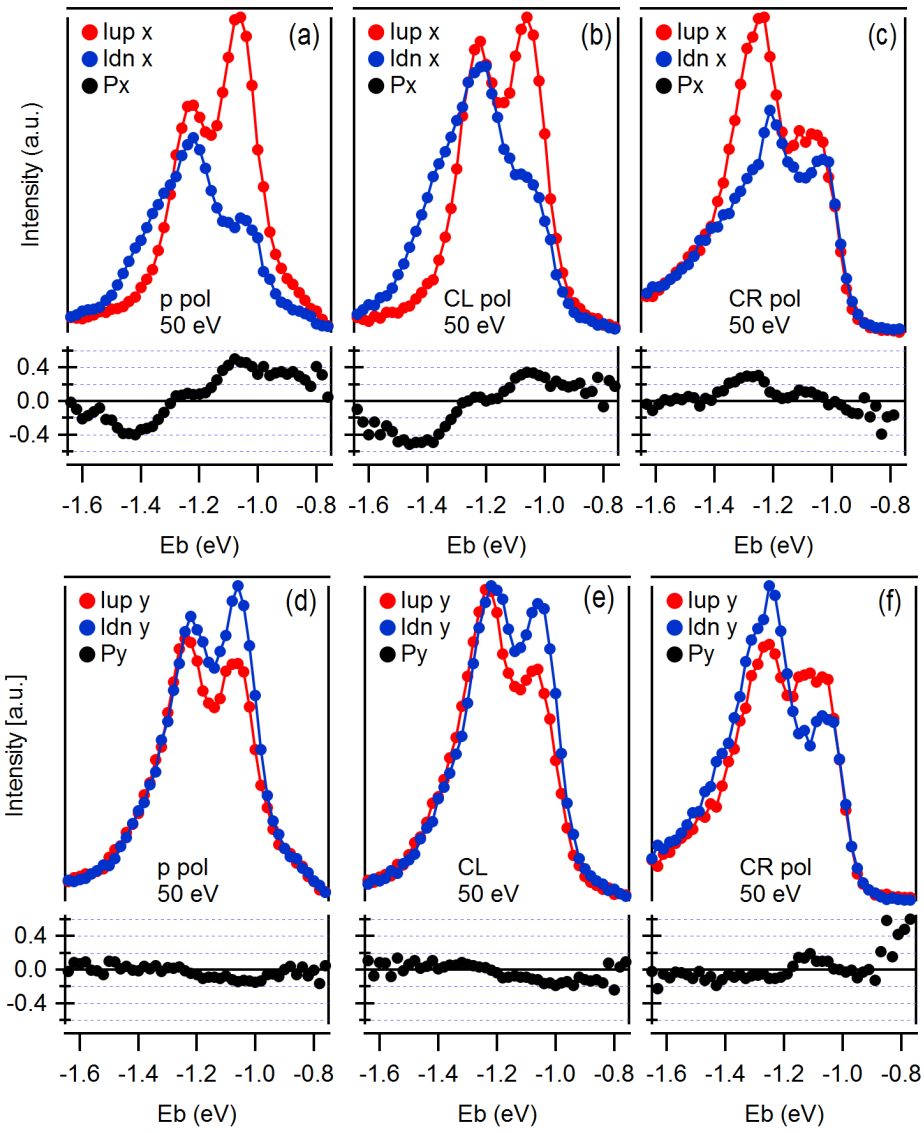

Figure 2: (a)-(f) Spin-resolved intensities (top) and spin polarization curves (bottom) at the $\overline{K}$-point along x (top row), y (bottom row) acquired at $h\nu = 50$ with $p-$, C_L and C_R polarized light.

2.9 Gaunt Coefficients

Now for the coefficient $g(l, m, l_k, m_k, L, M)$, they are the so-called Gaunt-coefficient,defined by the relation:

$$Y_l^m(\hat{r})Y_{l_k}^{m_k}(\hat{r}) = \sum_{L,M} g(l, m, l_k, m_k; L, M)Y_L^{M*}(\hat{r}). \tag{46}$$

In Condon-Shortley convention they are given by:

$$g(l, m, l_k, m_k; L, M) = \sqrt{\frac{(2l_k + 1)(2l + 1)}{4\pi(2L + 1)}}(-1)^M \langle l_k, m_k; l, m|l_k, l; L, -M\rangle \langle l_k, 0; l, 0|l_k, l; L, 0\rangle$$

where Clebsh-Gordan are defined as:

$$|j, m; l_1, l_2\rangle = \sum_{m_1,m_2} \langle l_1, m_1; l_2, m_2|l_1, l_2; j, m\rangle |l_1, m_1\rangle |l_2, m_2\rangle .$$

2.10 Photoemission from degenerate initial states

Given the set of degenerate wavefunctions Ψ_i bases of the sub-space relative to energy E. Any unitary linear combination of them, defined by a matrix $\mathbf{b}$:

$$|\Phi_j\rangle = \sum_i b_{ij} |\Psi_i\rangle \Leftrightarrow |\Psi_i\rangle = \sum_j b_{ij}^* |\Phi_j\rangle$$

leaves the photoemission intensity invariant. In fact:

$$\begin{aligned}
I \propto \sum_i |\langle \Psi_i|H_{int}|\Psi_{fin}\rangle|^2 &= \langle H_{int}\Psi_{fin}|\left(\sum_i |\Psi_i\rangle \langle \Psi_i|\right)|H_{int}\Psi_{fin}\rangle \\
&= \langle H_{int}\Psi_{fin}|\left(\sum_i \sum_{l,m} b_{i,l}^* |\Phi_l\rangle b_{i,m} \langle \Phi_m|\right)|H_{int}\Psi_{fin}\rangle \\
&= \langle H_{int}\Psi_{fin}|\left(\sum_{l,m} |\Phi_l\rangle \langle \Phi_m|\right)\left(\sum_i b_{i,l}^* b_{i,m}\right)|H_{int}\Psi_{fin}\rangle \\
&= \langle H_{int}\Psi_{fin}|\left(\sum_{l,m} |\Phi_l\rangle \langle \Phi_m|\right)\delta_{l,m}|H_{int}\Psi_{fin}\rangle \\
&= \sum_l |\langle \Phi_l|H_{int}|\Psi_{fin}\rangle|^2
\end{aligned}$$

where we used that $\mathbf{b}$ is unitary, i.e. $\mathbf{b}^\dagger\mathbf{b} = I$.

References

[1] V. N. Strocov, X. Wang, M. Shi, M. Kobayashi, J. Krempasky, C. Hess, T. Schmitt, and L. Patthey, *Soft-X-ray ARPES facility at the ADRESS beamline of the SLS: Concepts, technical realization and scientific applications*, J. Synchrotron Radiat. **21**, 32 (2014).

[2] A. Kuc, N. Zibouche, and T. Heine, *Influence of quantum confinement on the electronic structure of the transition metal sulfide TS_2*, Phys. Rev. B **83**, 245213 (2011).

[3] M. Hoesch , T. Greber , V.N. Petrov , M. Muntwiler , M. Hengsberger , W. Auwarter , J. Osterwalder, *Spin-polarized Fermi surface mapping*, Journal of Electron Spectroscopy and Related Phenomena **124** (2002) 263279.

[4] P. Blaha, K. Schwarz, G. Madsen, D. Kvasnicka and J. Luitz, WIEN2k, *An Augmented Plane Wave + Local Orbitals Program for Calculating Crystal Properties* (Karlheinz Schwarz, Techn. Universität Wien, Austria), 2001. ISBN 3-9501031-1-2

[5] G.-B. Liu, W.-Y. Shan, Y. Yao, W. Yao, and D. Xiao, *Three-band tight-binding model for monolayers of group-VIB transition metal dichalcogenides*, Phys. Rev. B **88**, 085433 (2013).

[6] F. Meier, V. Petrov, H. Mirhosseini , L. Patthey, J. Henk, J. Osterwalder and H. J. Dil, *Interference of spin states in photoemission from Sb/Ag(111) surface alloys*, J. Phys.: Condens. Matter **23**, 072207 (2011).

[7] D. Xiao, G.-B. Liu, W. Feng, X. Xu, and W. Yao, *Coupled Spin and Valley Physics in Monolayers of MoS_2 and Other Group-VI Dichalcogenides*, Phys. Rev. Lett. **108**, 196802 (2012).

[8] Z. Gong, G.-B. Liu, H. Yu, D. Xiao, X. Cui, X. Xu, and W. Yao *Magnetoelectric effects and valley-controlled spin quantum gates in transition metal dichalcogenide bilayers* Nat. Comm. **4**, 2053 (2013).

[9] M. Hamzavi, M. Movahedi, K.-E. Thylwe and A. A. Rajabi, *Approximate Analytical Solution of the Yukawa Potential with Arbitrary Angular Momenta*, Chin. Phys. Lett. **29**, 080302 (2012).